

# Revised upper limits for abundances of NH<sub>3</sub>, HCN and HC<sub>3</sub>N in the Martian atmosphere

A. Trokhimovskiy<sup>1</sup>, A. A. Fedorova<sup>1</sup>, F. Lefèvre<sup>2</sup>, O. Korablev<sup>1</sup>, K.S. Olsen<sup>3</sup>, J. Alday<sup>4</sup>,  
D. Belyaev<sup>1</sup>, F. Montmessin<sup>2</sup>, A. Patrakeev<sup>1</sup>, N. Kokonkov<sup>1</sup>

<sup>1</sup> Space Research Institute (IKI) RAS, Moscow, Russia

e-mail: trokh@cosmos.ru

<sup>2</sup> LATMOS/CNRS, Guyancourt, France

<sup>3</sup> Department of Physics, University of Oxford, Oxford, UK

<sup>4</sup> The Open University, Milton Keynes, UK

## Abstract

The Atmospheric Chemistry Suite (ACS) onboard the ExoMars Trace Gas Orbiter (TGO) spacecraft has been studying Mars' atmosphere since 2018. The sensitivity of the middle infrared channel (MIR) allows it to address many ardent topics and it is capable of improving and establishing upper limits for many trace species. In this work we present analysis of transmittance spectra in the 3332.5-3338.6 cm<sup>-1</sup> range with 30,000 resolution ( $\lambda/\Delta\lambda$ ), covering absorptions lines of three nitrogen-bearing species: ammonia (NH<sub>3</sub>), hydrogen cyanide (HCN) and cyanoacetylene (HC<sub>3</sub>N). According to existing models, all of those are not expected to be present in a CO<sub>2</sub>-rich Martian atmosphere, but outgassing or unknown chemistry sources cannot be discounted. The upper limits of 14, 1.5 and 11 ppbv are obtained for NH<sub>3</sub>, HCN and HC<sub>3</sub>N from individual occultation measurements during the warm and dusty perihelion season of martian year 36. For the ammonia and hydrogen cyanide the upper limits are improved compared to previously published results. A search for cyanoacetylene on Mars is reported for the first time.

**Keywords:** IR spectroscopy; Mars, atmosphere; Atmospheres, composition

## Main

Molecular nitrogen is the second most abundant species (2.8%) after CO<sub>2</sub> in the Martian atmosphere (Franz et al., 2017). Soil contains oxidised nitrogen-bearing compounds (Stern et al., 2015; Sutter et al., 2017). Also the chemically-derivatized molecules ammonia (NH<sub>3</sub>) and hydrogen cyanide (HCN) were detected from sand, among others, with the wet chemistry experiments of the Sample Analysis at Mars (SAM) instrument on NASA's Curiosity rover (Millan et al., 2022). The combination of an elevated abundance of derivatized ammonia and several N-bearing organic species detected in the follow-up analyses suggested that indigenous N-bearing molecules are present in the soil. At the same time, expected atmospheric processes involving nitrogen are limited (Lefèvre and Krasnopolsky, 2017), because the strong N–N bond makes N<sub>2</sub> a relatively inert species. Odd-nitrogen species, N and NO, can be produced as a result of N<sub>2</sub> dissociation at high altitudes only. The nitrogen chemistry in the lower atmosphere thus greatly depends on the downward fluxes. As calculated by the general circulation model of Moudden and McConnell (2007), main nitrogen species below 40 kilometres are NO and NO<sub>2</sub>, varying in tiny abundances from 0.1 ppbv to 0.25 ppbv. The current knowledge for NO<sub>2</sub> is <10 ppbv (Maguire, 1977) and less than 1.7 ppb for NO (Krasnopolsky, 2006). The sensitivity of the mid-infrared channel of the Atmospheric Chemistry Suite (ACS MIR) approaches the expected NO<sub>2</sub> 0.2 ppbv absorption features in the 2915 cm<sup>-1</sup>

48band, which will be a subject of a separate study. Not considering any release processes, other  
49nitrogen components are modelled to be orders of magnitude less abundant, like the pptv level  
50concentrations of  $\text{HNO}_4$  near 20 km in altitude.

51 In this work we present upper limits of somewhat unexpected molecules for Mars:  
52ammonia, hydrogen cyanide and cyanoacetylene derived from ACS MIR data. The first two  
53have been already searched for on Mars, the third has not yet been considered.

54 As in the case of methane ( $\text{CH}_4$ ), the ammonia could be considered as a biomarker. But  
55in contrast to methane, whose lifetime is considered to be on the order of a hundred years  
56(Lefèvre and Krasnopolsky, 2017), ammonia is not a stable molecule in the atmosphere of Mars  
57and would be quickly photolyzed within hours. Hydrogen cyanide is also not expected to be  
58produced in the Martian atmosphere (Mancinelli and Banin, 2003): its permanent presence  
59would require a continuous source, like active volcanoes or biota, both actively sought, but  
60never detected on Mars.

61 The first  $\text{NH}_3$  3  $\sigma$  upper limit of 8 ppbv was set by the Mariner 9 Infrared Interferometer  
62Spectrometer (IRIS; Maguire, 1977). The results were obtained from an average of spectra  
63from all over the planet, covering a full Martian year (MY), starting from  $L_s = 293^\circ$  in MY 9. In  
642004, the detection of ammonia in the atmosphere of Mars by the Planetary Fourier  
65Spectrometer (PFS) was announced; the report was not followed by a publication. The  $\text{NH}_3$   
66was then sought using NIRSPEC at Keck-2 observatory (Villanueva et al., 2013). The  
67observations at  $L_s = 352^\circ$  in MY 27 provided a 57 ppbv 3  $\sigma$  upper limit, and at  $L_s = 83^\circ$  in MY  
6830, a 45 ppbv upper limit. In parallel, they have established HCN upper limits of 4.5 and 2.1  
69ppbv, respectively.

70  $\text{HC}_3\text{N}$  was not considered as a goal for Martian atmospheric surveys, while it has a  
71notable astrochemical importance (e.g. Thelen et al., 2019; Jiang et al., 2017). The most recent  
72version of the spectroscopy database HITRAN2020 (Gordon et al., 2022) includes, for the first  
73time, ro-vibrational transitions relative to all seven vibrational modes of  $\text{HC}_3\text{N}$  up to  $3400\text{ cm}^{-1}$ ,  
74and rotational data in the ground state and many vibrational states of all normal modes. In this  
75work, we used the recently documented band around  $3327\text{ cm}^{-1}$  to set the first upper limit on  
76 $\text{HC}_3\text{N}$  in Mars atmosphere.

77 The ACS package for the Trace Gas Orbiter (TGO) is a part of the ExoMars mission  
78(Korablev et al., 2018; Vago et al., 2015). ACS includes the mid-infrared channel (MIR), a  
79versatile instrument for the spectral range  $2.3\text{--}4.2\text{ }\mu\text{m}$ . It is a cross-dispersion echelle  
80instrument dedicated to solar occultation measurements. The resolving power of 30,000 and a  
81signal-to-noise ratio (SNR) of 5,000 per pixel per 2 s acquisition make it perfect for detecting  
82weak absorptions (Trokhimovskiy et al., 2020; Olsen et al., 2020). We use the ACS MIR  
83measurements obtained using secondary grating position 13, which includes 27 diffraction  
84orders (190–216) encompassing a spectral range of  $3178\text{--}3643\text{ cm}^{-1}$ . Order 199 covers a range  
85 $3330.5\text{--}3355.1\text{ cm}^{-1}$ , where all three gases,  $\text{NH}_3$ , HCN, and  $\text{HC}_3\text{N}$ , have absorption lines. This  
86range also contains  $\text{CO}_2$  and  $\text{H}_2\text{O}$  lines, which are used for additional pixel-to-wavenumber  
87calibration. To retrieve upper limits in this work, we used a narrower  $3332.5\text{--}3338.6\text{ cm}^{-1}$  fitting  
88window (see Figure 1 Panel A for model spectra of sought gases and data example).

89 Regular and optimised position 13 measurements have started mid MY 36. The dataset  
90analysed includes 135 ACS MIR occultations performed in MY 36 during southern summer at  
91the perihelion season ( $L_s = 212^\circ\text{--}360^\circ$ ; TGO orbits 19,656–22,705). The observation period is  
92characterised by greater dust load, higher temperatures, elevation of water vapour up to  
93120 km (Belyaev et al., 2021; Fedorova et al., 2023). Recently discovered by ACS, hydrogen  
94chloride is being observed exceptionally in the perihelion season (Korablev et al., 2021; Olsen  
95et al., 2021), emphasising more active atmospheric chemistry. The observed latitudes range

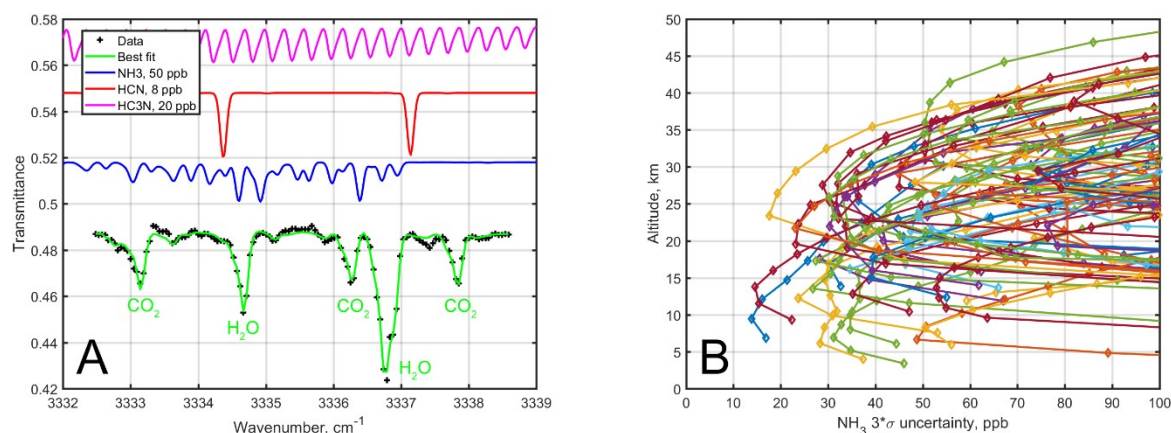
96 from  $-77^{\circ}\text{S}$  to  $90^{\circ}\text{N}$ , with the majority of occultations occurring at high latitudes (Korablev et al., 97 2018).

98 The retrieval is performed by the iterative Levenberg–Marquardt iterative algorithm with  
99 Tikhonov regularisation developed to analyse data from SPICAM IR spectrometer on Mars  
100 Express (Fedorova et al., 2018) and TGO's ACS near-infrared channel (NIR) data (Fedorova et  
101 al., 2020) and adapted for ACS MIR data (Trokhimovskiy et al., 2021; Fedorova et al., 2022).  
102 The  $\text{CO}_2$  density and temperature profiles were not retrieved, but taken from ACS NIR  
103 simultaneous measurements (Korablev et al., 2018; Fedorova et al., 2023). The free  
104 parameters are aerosol extinction and volume mixing ratios of gases. In the absence of  
105 detection, the uncertainty on the retrieved quantities is given by the covariance matrix of the  
106 solution, which defines the upper limit. The retrieved values are generally within a  $1\sigma$  away  
107 from zero; we present the three-sigma upper limits as a confident non-detection case. The  
108 vertical dependence of the upper limits is typical for occultation experiments and for Mars  
109 reaches the best values at altitudes of about 10–25 km. At higher altitudes, the line-of-sight  
110 captures only a miserable number of searched molecules, at lower altitudes the signal is  
111 diminished by aerosol load. On Figure 1 Panel B we present a collection of three-sigma upper  
112 limits for  $\text{NH}_3$  from different orbits. The vertical pattern for HCN and  $\text{HC}_3\text{N}$  is similar.

113 The best upper limits are achieved at  $L_s = 233^{\circ}$ , latitude  $64^{\circ}\text{N}$  and altitude 10 km, and  
114 accordingly for  $\text{NH}_3$ , HCN and  $\text{HC}_3\text{N}$  are 14, 1.5 and 11 ppbv. Tens of observations provide  
115 upper limits below 33, 3.5 and 30 ppbv at high latitudes in both hemispheres during the whole  
116 season observed. The upper limit for  $\text{HC}_3\text{N}$  is not restrictive since HCN is typically the most  
117 abundant nitrile. At lower latitudes, with more aerosols and less occultations available, the best  
118 upper limits by ACS MIR for  $\text{NH}_3$ , HCN and  $\text{HC}_3\text{N}$  were 114, 12 and 95 ppbv. These numbers  
119 were achieved at  $L_s = 287^{\circ}$ , latitude  $-12^{\circ}\text{S}$  and altitude 39 km.

120 The upper limits for ammonia and hydrogen cyanide are several times below those  
121 obtained by Villanueva et al. (2013) for the end of MY 27. Moreover, the ACS data cover the  
122 entire perihelion season and different latitudes. The upper limits for cyanoacetylene in the  
123 Martian atmosphere are obtained for the first time. Tracing these species, unexpected on Mars,  
124 with stringent upper limits is important to monitor potential outgassing events and constrain  
125 chemical models. As the ExoMars mission continues, ACS will extend the trace species search  
126 further.

127



128  
129

130 Figure 1. Panel A. Example of ACS MIR data from order 199 and the best fit at tangent  
131 altitude 18 km, orbit 21352 N1,  $L_s = 299^{\circ}$ , latitude  $-55^{\circ}\text{S}$ . The model spectra for  $\text{NH}_3$ , HCN and  
132  $\text{HC}_3\text{N}$  are shown shifted and with abundances of 50, 8 and 20 ppbv, respectively. The

133noticeable lines fitted in the data are due to CO<sub>2</sub> and are located at 3333.1, 3336.2 and 3337.8  
134cm<sup>-1</sup>, the H<sub>2</sub>O line is at 3334.6 cm<sup>-1</sup> and a doublet around 3336.8 cm<sup>-1</sup>. Panel B. The vertical  
135dependency of the three-sigma upper limits for ammonia from the ACS MIR solar occultation  
136observations. The vertical pattern for HCN and HC<sub>3</sub>N is similar. Different colours stand for  
137distinct occultations.

138

139

140Belyaev, D., Fedorova, A.A., Trokhimovskiy, A., Alday, J., Montmessin, F., Korablev, O.I.,  
141 Lefèvre, F., Patrakeev, A.S., Olsen, K.S., Shakun, A.V., 2021. Revealing a high water  
142 abundance in the upper mesosphere of Mars with ACS onboard TGO. *J. Geophys. Res.*  
143 *Letters*, Volume48, Issue10. <https://doi.org/10.1029/2021GL093411>

144Franz, H.B. et al. 2017. Initial SAM calibration gas experiments on Mars: Quadrupole mass  
145 spectrometer results and implications. *Planetary and Space Science* 138, 44–54.  
146 [doi:10.1016/j.pss.2017.01.014](https://doi.org/10.1016/j.pss.2017.01.014)

147Fedorova, A., Bertaux, J.-L., Betsis, D., Montmessin, F., Korablev, O., Maltagliati, L., Clarke,  
148 J., 2018. Water vapor in the middle atmosphere of Mars during the 2007 global dust  
149 storm. *Icarus*. 300, pp. 440-457. <https://doi.org/10.1016/j.icarus.2017.09.025>.

150Fedorova, A.A., Montmessin, F., Korablev, O., Luginin, M., Trokhimovskiy, A., Belyaev, D.A.,  
151 Ignatiev, N.I., Lefèvre, F., Alday, J., Irwin, P.G.J., Olsen, K.S., Bertaux, J.-L., Millour, E.,  
152 Määttänen, A., Shakun, A., Grigoriev, A.V., Patrakeev, A., Korsas, S., Kokonkov, N.,  
153 Baggio, L., Forget, F., Wilson, C.F., 2020. Stormy water on Mars: The distribution and  
154 saturation of atmospheric water during the dusty season. *Science*. 367, pp. 297-300.  
155 <https://doi.org/10.1126/science.aay9522>.

156Fedorova, A., Trokhimovskiy, A., Lefèvre, F., Olsen, K.S., Korablev, O., Montmessin, F.,  
157 Ignatiev, N., Lomakin, A., Forget, F., Belyaev, D., Alday, J., Luginin, M., Smith, M.,  
158 Patrakeev, A., Shakun, A., Grigoriev, A., 2022. Climatology of the CO vertical distribution  
159 on Mars based on ACS TGO measurements. *J. Geophys. Res.: Planets*. 127,  
160 e2022JE007195. <https://doi.org/10.1029/2022JE007195>.

161Fedorova, A.A., Montmessin, F., Trokhimovskiy, A., Luginin, M., Korablev, O., Alday, J.,  
162 Belyaev, D., Holmes, J., Lefevre, F., Olsen, K., Patrakeev, A., Shakun, F. 2023. A two-  
163 martian years survey of the water vapor saturation state on Mars based on ACS  
164 NIR/TGO occultations. *J. Geophys. Res.: Planets*. e2022JE007348.  
165 <https://doi.org/10.1029/2022JE007348>

166Gordon, I.E., Rothman, L.S., Hargreaves, R.J., Hashemi, R., Karlovets, E.V., Skinner, F.M.,  
167 Conway, E.K., Hill, C., Kochanov, R.V., Tan, Y., Wcisło, P., Finenko, A.A., Nelson, K.,  
168 Bernath, P.F., Birk, M., Boudon, V., Campargue, A., Chance, K.V., Coustenis, A., Drouin,  
169 B.J., Flaud, J.-M., Gamache, R.R., Hodges, J.T., Jacquemart, D., Mlawer, E.J., Nikitin,  
170 A.V., Perevalov, V.I., Rotger, M., Tennyson, J., Toon, G.C., Tran, H., Tyuterev, V.G.,  
171 Adkins, E.M., Baker, A., Barbe, A., Canè, E., Császár, A.G., Dudaryonok, A., Egorov, O.,  
172 Fleisher, A.J., Fleurbaey, H., Foltynowicz, A., Furtenbacher, T., Harrison, J.J., Hartmann,  
173 J.-M., Horneman, V.-M., Huang, X., Karman, T., Karns, J., Kassi, S., Kleiner, I., Kofman,  
174 V., Kwabia-Tchana, F., Lavrentieva, N.N., Lee, T.J., Long, D.A., Lukashevskaya, A.A.,  
175 Lyulin, O.M., Makhnev, V.Yu., Matt, W., Massie, S.T., Melosso, M., Mikhailenko, S.N.,  
176 Mondelain, D., Müller, H.S.P., Naumenko, O.V., Perrin, A., Polyansky, O.L., Raddaoui, E.,  
177 Raston, P.L., Reed, Z.D., Rey, M., Richard, C., Tóbiás, R., Sadiek, I., Schwenke, D.W.,  
178 Starikova, E., Sung, K., Tamassia, F., Tashkun, S.A., Vander Auwera, J., Vasilenko, I.A.,  
179 Vigasin, A.A., Villanueva, G.L., Vispoe, B., Wagner, G., Yachmenev, A., Yurchenko,

180 S.N., 2022. The HITRAN2020 molecular spectroscopic database. J.Q.S.R.T. 277,  
 181 107949. <https://doi.org/10.1016/j.jqsrt.2021.107949>.

182 Jiang, X.-J., Wang, J.-Z., Gao Y., Gu, Q.-S., 2017. HC3N observations of nearby galaxies.  
 183 A&A. 600, A15. <https://doi.org/10.1051/0004-6361/201629066>.

184 Korablev, O., Montmessin, F., Trokhimovskiy, A., Fedorova, A.A., Shakun, A.V., Grigoriev,  
 185 A.V., Moshkin, B.E., Ignatiev, N.I., Forget, F., Lefèvre, F., Anufreychik, K., Dzuban, I.,  
 186 Ivanov, Y.S., Kalinnikov, Y.K., Kozlova, T.O., Kungurov, A., Makarov, V., Martynovich, F.,  
 187 Maslov, I., Merzlyakov, D., Moiseev, P.P., Nikolskiy, Y., Patrakeeve, A., Patsaev, D.,  
 188 Santos-Skripko, A., Sazonov, O., Semena, N., Semenov, A., Shashkin, V., Sidorov, A.,  
 189 Stepanov, A. V., Stupin, I., Timonin, D., Titov, A.Y., Viktorov, A., Zharkov, A., Altieri, F.,  
 190 Arnold, G., Belyaev, D.A., Bertaux, J. L., Betsis, D.S., Duxbury, N., Encrenaz, T.,  
 191 Fouchet, T., Gérard, J.-C., Grassi, D., Guerlet, S., Hartogh, P., Kasaba, Y., Khatuntsev,  
 192 I., Krasnopolsky, V.A., Kuzmin, R.O., Lellouch, E., Lopez-Valverde, M.A., Luginin, M.,  
 193 Määttänen, A., Marcq, E., Martin Torres, J., Medvedev, A.S., Millour, E., Olsen, K.S.,  
 194 Patel, M.R., Quantin-Nataf, C., Rodin, A.V., Shematovich, V.I., Berkenboschs, I.,  
 195 Thomas, N., Vazquez, L., Vincendon, M., Wilquet, V., Wilson, C.F., Zasova, L.V., Zelenyi,  
 196 L.M., Zorzano, M.P., 2018. The Atmospheric Chemistry Suite (ACS) of Three  
 197 Spectrometers for the ExoMars 2016 Trace Gas Orbiter. Space Sci. Rev. 214, 7.  
 198 <https://doi.org/10.1007/s11214-017-0437-6>.

199 Korablev, O., Olsen, K.S., Trokhimovskiy, A., Lefèvre, F., Montmessin, F., Fedorova, A.A.,  
 200 Toplis, M.J., Alday, J., Belyaev, D.A., Patrakeeve, A., Ignatiev, N.I., Shakun, A.V.,  
 201 Grigoriev, A.V., Baggio, L., Abdenour, I., Lacombe, G., Ivanov, Y.S., Aoki, S., Thomas,  
 202 I.R., Daerden, F., Ristic, B., Erwin, J.T., Patel, M., Bellucci, G., Lopez-Moreno, J.-J.,  
 203 Vandaele, A.C., 2021. Transient HCl in the atmosphere of Mars. Sci. Adv. 7, eabe4386.  
 204 <https://doi.org/10.1126/sciadv.abe4386>.

205 Krasnopolsky, V.A. 2006. A sensitive search for nitric oxide in the lower atmospheres of Venus  
 206 and Mars: Detection on Venus and upper limit for Mars. Icarus 182, 80–91.  
 207 doi:10.1016/j.icarus.2005.12.003

208 Lefèvre, F., Krasnopolsky, V., 2017. Atmospheric Photochemistry. In: Haberle, R.M., Clancy,  
 209 R.T., Forget, F., Smith, M.D., Zurek, R.W. (Eds.), The Atmosphere and Climate of Mars,  
 210 pp. 405 - 432. <http://dx.doi.org/10.1017/9781139060172.013>.

211 Maguire, W.C., 1977. Martian isotopic ratios and upper limits for possible minor constituents as  
 212 derived from Mariner 9 infrared spectrometer data. Icarus. 32, pp. 85–97.  
 213 [https://doi.org/10.1016/0019-1035\(77\)90051-3](https://doi.org/10.1016/0019-1035(77)90051-3).

214 Mancinelli, R.L., Banin, A., 2003. Where is the nitrogen on Mars? Int. J. Astrobiol. 2, pp. 217–  
 215 225. <https://doi.org/10.1017/S1473550403001599>.

216 Millan, M., Teinturier, S., Malespin, C.A., Bonnet, J.Y., Buch, A., Dworkin, J.P., Eigenbrode,  
 217 J.L., Freissinet, C., Glavin, D.P., Navarro-González, R., Srivastava, A., Stern, J.C., Sutter,  
 218 B., Szopa, C., Williams, A.J., Williams, R.H., Wong, G.M., Johnson, S.S., Mahaffy, P. R.,  
 219 2022. Organic molecules revealed in Mars's Bagnold Dunes by Curiosity's derivatization  
 220 experiment. Nat. Astron. 6, pp. 129–140. <https://doi.org/10.1038/s41550-021-01507-9>.

221 Montmessin, F., Korablev, O.I., Trokhimovskiy, A., Lefèvre, F., Fedorova, A.A., Baggio, L.,  
 222 Irbah, A., Lacombe, G., Olsen, K.S., Braude, A.S., Belyaev, D.A., Alday, J., Forget, F.,  
 223 Daerden, F., Pla-Garcia, J., Rafkin, S., Wilson, C.F., Patrakeeve, A., Shakun, A., Bertaux,  
 224 J.L., 2021. A stringent upper limit of 20 pptv for methane on Mars and constraints on its  
 225 dispersion outside Gale crater. A&A. 650, A140. [https://doi.org/10.1051/0004-](https://doi.org/10.1051/0004-6361/202140389)  
 226 6361/202140389.

227Moudden Y., McConnell, J.C., 2007. Three-dimensional on-line chemical modelling in a Mars  
 228 general circulation model. *Icarus*. 188, pp. 18-34.  
 229 <http://dx.doi.org/10.1016/j.icarus.2006.11.005>.

230Olsen, K.S., Lefèvre, F., Montmessin, F., Trokhimovskiy, A., Baggio, L., Fedorova, A.A., Alday,  
 231 J., Lomakin, A., Belyaev, D.A., Patrakeev, A., Shakun, A., Korablev, O.I., 2020. First  
 232 detection of ozone in the mid-infrared at Mars: implications for methane detection. *A.&A.*  
 233 639, A141. <https://doi.org/10.1051/0004-6361/202038125>.

234Olsen, K.S., Trokhimovskiy, A., Montabone, L., Fedorova, A.A., Luginin, M., Lefèvre, F.,  
 235 Korablev, O.I., Montmessin, F., Forget, F., Millour, E., Bierjon, A., Baggio, L., Alday, J.,  
 236 Wilson, C.F., Irwin, P.G.J., Belyaev, D.A., Patrakeev, A., Shakun, A., 2021. Seasonal  
 237 reappearance of HCl in the atmosphere of Mars year 35 dusty season. *A.&A.* 647, A161.  
 238 <https://dx.doi.org/10.1051/0004-6361/202140329>.

239Stern, J.C., Sutter, B., Freissinet, C., Navarro-González, R., McKay, C.P., Archer Jr., P.D.,  
 240 Buch, A., Brunner, A.E., Coll, P., Eigenbrode, J.L., Fairen, A.G., Franz, H.B., Glavin, D.P.,  
 241 Kashyap, S., McAdam, A.C., Ming, D.W., Steele, A., Szopa, C., Wray, J.J., Martín-Torres,  
 242 F.J., Zorzano, M.-P., Conrad, P.G., Mahaffy, P.R. and the MSL Science Team, 2015.  
 243 Evidence for indigenous nitrogen in sedimentary and aeolian deposits from the Curiosity  
 244 rover investigations at Gale crater, Mars. *PNAS*. 112, pp. 4245-4250.  
 245 <https://doi.org/10.1073/pnas.1420932112>.

246Sutter, B., McAdam, A.C., Mahaffy, P.R., Ming, D.W., Edgett, K.S., Rampe, E.B., Eigenbrode,  
 247 J.L., Franz, H.B., Freissinet, C., Grotzinger, J.P., Steele, A., House, C.H., Archer, P.D.,  
 248 Malespin, C.A., Navarro-González, R., Stern, J.C., Bell, J.F., Calef, F.J., Gellert, R.,  
 249 Glavin, D.P., Thompson, L.M., Yen, A.S., 2017. Evolved gas analyses of sedimentary  
 250 rocks and eolian sediment in Gale Crater, Mars: Results of the Curiosity rover's sample  
 251 analysis at Mars instrument from Yellowknife Bay to the Namib Dune. *J. Geophys. Res.*  
 252 *Planets*. 122, pp. 2574-2609. <https://doi.org/10.1002/2016JE005225>.

253Thelen, A.E., Nixon, C.A., Chanover, N.J., Cordiner, M.A., Molter, E.M., Teanby, N.A., Irwin,  
 254 P.G.J., Serigano, J., Charnley, S.B., 2019. Abundance measurements of Titan's  
 255 stratospheric HCN, HC3N, C3H4, and CH3CN from ALMA observations. *Icarus*. 319, pp.  
 256 417-432. <https://doi.org/10.1016/j.icarus.2018.09.023>.

257Trokhimovskiy, A., Perevalov, V., Korablev, O., Fedorova, A.A., Olsen, K.S., Bertaux, J.-L.,  
 258 Patrakeev, A., Shakun, A., Montmessin, F., Lefèvre, F., Lukashevskaya, A., 2020. First  
 259 observation of the magnetic dipole CO<sub>2</sub> main isotopologue absorption band at 3.3  $\mu$ m in  
 260 the atmosphere of Mars by ExoMars Trace Gas Orbiter ACS instrument. *A.&A.* 639,  
 261 A142. <https://dx.doi.org/10.1051/0004-6361/202038134>.

262Trokhimovskiy, A., Fedorova, A.A., Olsen, K.S., Alday, J., Korablev, O., Montmessin, F.,  
 263 Lefèvre, F., Patrakeev, A., Belyaev, D., Shakun, A.V., 2021. Isotopes of chlorine from HCl  
 264 in the Martian atmosphere. *A. & A.* 651, A32. <https://doi.org/10.1051/0004-6361/202140916>.

266Vago, J., Witasse, O., Svedhem, H., Baglioni, P., Haldemann, A., Gianfiglio, G., Blancquaert,  
 267 T., McCoy, D., de Groot, R., 2015. ESA ExoMars program: The next step in exploring  
 268 Mars. *Sol. Sys. Res.* 49, pp. 518-528. <https://doi.org/10.1134/S0038094615070199>.

269Villanueva, G.L., Mumma, M.J., Novak, R.E., Radeva, Y.L., Käufl, H.U., Smette, A., Tokunaga,  
 270 A., Khayat, A., Encrenaz, T., Hartogh, P., 2013. A sensitive search for organics (CH<sub>4</sub>,  
 271 CH<sub>3</sub>OH, H<sub>2</sub>CO, C<sub>2</sub>H<sub>6</sub>, C<sub>2</sub>H<sub>2</sub>, C<sub>2</sub>H<sub>4</sub>), hydroperoxyl (HO<sub>2</sub>), nitrogen compounds (N<sub>2</sub>O,  
 272 NH<sub>3</sub>, HCN) and chlorine species (HCl, CH<sub>3</sub>Cl) on Mars using ground-based high-  
 273 resolution infrared spectroscopy. *Icarus*. 223, pp. 11-27.  
 274 <https://doi.org/10.1016/j.icarus.2012.11.013>.

275  
276  
277  
278  
279